

Fragment Flow in Nuclear Collisions

K. G. R. Doss,^{(1),(a)} H.-A. Gustafsson,^{(2),(b)} H. Gutbrod,⁽²⁾ J. W. Harris,⁽¹⁾ B. V. Jacak,⁽³⁾ K.-H. Kampert,^{(2),(c)} B. Kolb,⁽²⁾ A. M. Poskanzer,⁽¹⁾ H.-G. Ritter,⁽¹⁾ H. R. Schmidt,⁽²⁾ L. Teitelbaum,⁽¹⁾ M. Tincknell,⁽¹⁾ S. Weiss,⁽¹⁾ and H. Wieman⁽¹⁾

⁽¹⁾Lawrence Berkeley Laboratory, University of California, Berkeley, California 94720

⁽²⁾Gesellschaft für Schwerionenforschung, Darmstadt, West Germany

⁽³⁾Los Alamos National Laboratory, Los Alamos, New Mexico 87545

(Received 30 July 1987)

The flow of light nuclei ($Z=1,2$) and intermediate-mass nuclear fragments ($3 \leq Z < 10$) is measured in collisions of 200-MeV/nucleon Au+Au over a large solid angle. An increase in the fragment-position and momentum-space alignment relative to the reaction plane is observed: The fragments exhibit stronger flow effects than light particles.

PACS numbers: 25.70.Np

A collective sideways flow of light particles ($Z=1,2$) has recently been observed in relativistic nucleus-nucleus collisions.^{1,2} Initially predicted by theoretical fluid dynamics,³⁻⁵ collective flow also arises in various other models⁶⁻⁹ incorporating compressional degrees of freedom in the form of a pressure-density relation, i.e., an equation of state. In these models the amount of transverse flow is directly related to the stiffness of the nuclear equation of state and transport properties of the nuclear medium.¹⁰ As two incident nuclei collide, the pressure and density increase in the interaction region. At nonzero impact parameters there is an inherent asymmetry in the pressure, which results in a transverse flow of matter in the directions of lowest pressure. Several calculations,¹¹⁻¹³ capable of producing nuclear fragments ($Z > 2$), predict that a stronger collective-flow effect should be observed for nuclear fragments than light particles emitted in the reaction. Previous experiments identifying heavier fragments have only studied single-fragment inclusive distributions or correlations¹⁴ other than fragment flow. In this Letter we present results from a large-solid-angle study¹⁵ of the production of light particles ($Z=1,2$) and intermediate-mass fragments ($3 \leq Z \leq 9$), and provide the first conclusive evidence that the fragments exhibit stronger flow effects than light particles.

The Gesellschaft für Schwerionenforschung Darmstadt mbH/Lawrence Berkeley Laboratory Plastic Ball/Wall detector system¹⁶ was used to study light and intermediate-mass fragments over a large solid angle in 200-MeV/nucleon Au+Au reactions at the Bevalac. The Plastic Ball consists of 815 CaF₂ (ΔE)-plastic-scintillator (E) telescope modules covering the angular region from $10^\circ \leq \theta_{\text{lab}} \leq 160^\circ$ with H and He isotope identification.

Computer-controlled high-voltage modules were implemented on the 160 Ball modules at $\theta_{\text{lab}} \leq 30^\circ$, to enable on-line gain matching. With a careful reduction in gain for these forward Ball modules, their dynamic range

was extended, enabling the simultaneous measurement of all produced nuclei from H to Ne. Unit separation of nuclear charges for $1 \leq Z < 10$ was obtained with isotope separation for $Z=1$ and 2.¹⁵ A calibration for the fragment charge identification was made by detection of low-energy ¹²C beams and ¹²C fragmentation products at the Bevalac with time-of-flight techniques. In order to be identified, fragments were required to traverse the 4-mm-thick CaF₂ ΔE scintillator producing a low-energy cutoff in the laboratory of $E_{\text{lab}} \approx 35-40$ MeV/nucleon. Since the velocity of the c.m. system corresponds to $E_{\text{lab}} \approx 50$ MeV/nucleon energy, the low-energy cutoff is unimportant in the forward direction of the c.m. system. The measurements of intermediate-mass fragments were only performed at $\theta_{\text{lab}} \leq 30^\circ$ which corresponds mainly to the forward hemisphere in the c.m. The Plastic Wall covers angles $\theta_{\text{lab}} < 10^\circ$ with sixty pairs of scintillation counters, providing particle identification for $1 \leq Z \leq 6$ and velocities $\beta \geq 0.3$ (45 MeV/nucleon) via time of flight and energy loss. The acceptance for light charged particles extends over 4π allowing each event to be characterized by charged-particle multiplicity. In addition, there was a zero-degree gas proportional chamber¹⁷ covering $0^\circ \pm 2^\circ$ in the laboratory. This detector with its five wire planes enabled extremely high position resolution for large projectiles remnants. Beam-defining counters employing standard pileup rejection techniques were used to ensure against chance-coincidence events.¹⁶

Multiplicity distributions of fragments with $3 \leq Z < 10$, observed in the forward hemisphere of the c.m. frame, are displayed in Fig. 1. Events are sorted according to participant-proton multiplicity as defined by Doss *et al.*,¹⁸ including protons bound in H and He isotopes. The multiplicity bins used are $0 < M \leq 23$, $23 < M \leq 46$, $46 < M \leq 69$, $69 < M \leq 92$, and $M > 92$. These multiplicity bins are labeled MUL1, MUL2, MUL3, MUL4, and MUL5, respectively, and range from peripheral collisions with few observed charges to central collisions with very high multiplicities. As seen in Fig. 1,

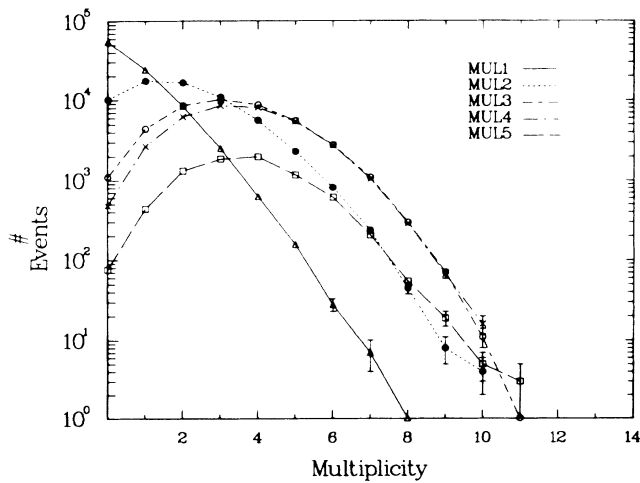


FIG. 1. Fragment ($Z \geq 3$) multiplicity distributions for 200-MeV/nucleon Au+Au for five participant proton multiplicity bins increasing from MUL1 to MUL5. These multiplicities correspond to fragments emitted in the forward hemisphere of the c.m. system.

most peripheral collisions (MUL1) result in a low multiplicity of intermediate-mass fragments. These fragments are observed to have energies close to that of the projectile, and a large projectile remnant is usually observed in the zero-degree detector. Smaller remnants are observed as the charge multiplicity increases, corresponding to decrease impact parameter.

In central collisions (MUL4 and MUL5) practically all of the projectile charge is observed in light- and intermediate-mass fragments at midrapidity, with no large projectile remnant remaining. As seen in Fig. 1 there are on the average three to four fragments per event at $\theta_{c.m.} \leq 90^\circ$ for central collisions. Extrapolation to 4π leads to eight or more intermediate-mass fragments in central collisions, with a significant number of events producing as many as twenty fragments. These numbers are slight underestimates because of the low- β cutoff for fragments. However, the total charge measured for $\theta_{c.m.} \leq 90^\circ$ in these two multiplicity bins sums to 80% to 90% of the projectile charge signifying that most of the fragments are observed.

In order to study the flow of fragments, the transverse-momentum analysis technique¹⁹ was employed to determine the reaction plane of each event. In this method the vector difference of the transverse-momentum components of particles going forward and those going backwards in the c.m. is used together with the beam axis to define the reaction plane. This difference corresponds to the collective transverse-momentum transfer in the c.m. The transverse momentum p_\perp of each particle is then projected onto the reaction plane, where the particle of interest has been excluded from determination of the plane (i.e., autocorrelations are removed), yielding the in-plane transverse momentum p_x . For each particle, the

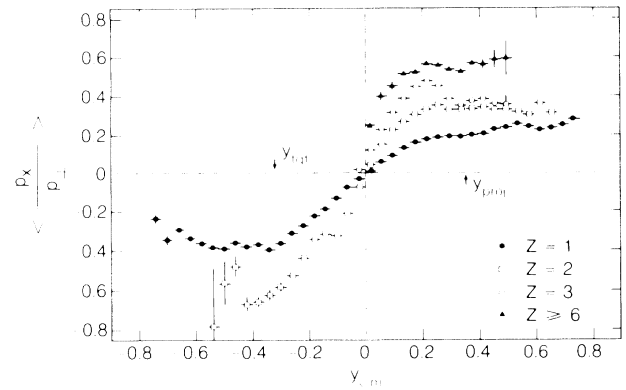


FIG. 2. The mean value of the transverse momentum projected onto the reaction plane (defined in text) divided by the transverse-momentum vector modulus as a function of c.m. rapidity for 200-MeV/nucleon Au+Au. Displayed are the values for $Z=1, 2, 3$ and $Z \geq 6$.

fraction of the particle's transverse momentum that lies in the reaction plane is calculated. Displayed in Fig. 2 is the mean value of the transverse-momentum alignment $\langle p_x/p_\perp \rangle$ in the MUL3 multiplicity bin for particles as a function of their rapidity for $Z=1, 2, 3$, and 6. Positive and negative values of $\langle p_x/p_\perp \rangle$ correspond to emission projected into the reaction plane, but on opposite sides. The forward-backward asymmetry is an artifact of experimental biases at low particle energies (near target rapidity) and spectator cuts in the projectile rapidity region made using the prescription of Ref. 18. Since participant-spectator discrimination is not unique, the slopes of the curves at midrapidity in Fig. 2 best characterize the flow.²⁰ Figure 2 clearly shows that an increasingly larger part of the fragment's transverse momentum lies in the reaction plane as the fragment mass increases. The $Z=3, 6$ fragments are more aligned in the plane than the $Z=1, 2$ particles which are interpreted to flow collectively.^{1, 2, 6-9, 19} Furthermore, the absolute value of the transverse momentum per nucleon projected into the reaction plane is observed to increase weakly with fragment mass.²¹

Having studied the alignment of fragments in momentum space, the spatial correlation of the fragments with the reaction plane will now be examined. Presented in Fig. 3 are directivity plots showing the azimuthal correlation of emitted light particles and fragments with the reaction plane. The angle plotted is the azimuthal emission angle of each particle or fragment with respect to the reaction plane defined by the $Z=1, 2$ light particles with autocorrelations removed. The left-hand column labeled MUL2 contains relatively peripheral collisions, and the right-hand column, MUL4, relatively central ones. Collisions at extremely large or small impact parameters result in poorly defined reaction planes and are not shown here. The two curves in each box correspond

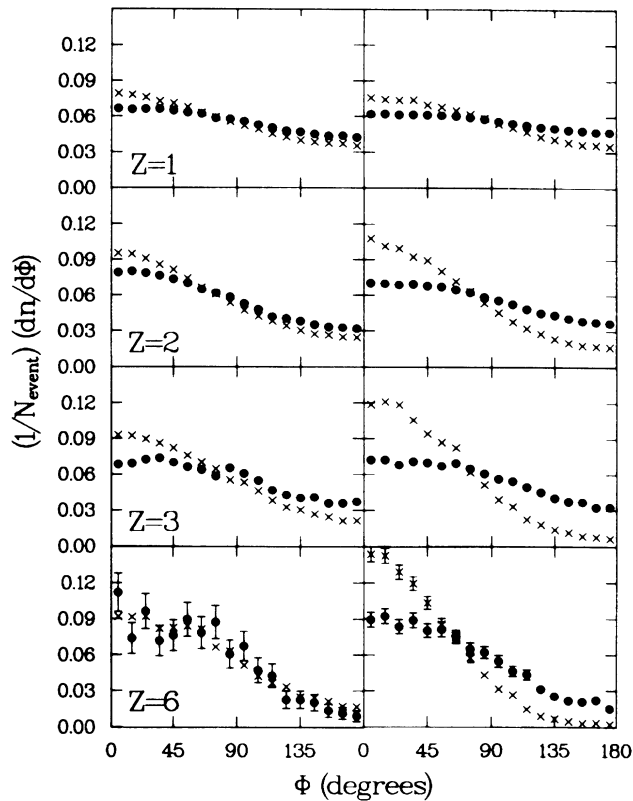


FIG. 3. Directivity plots (azimuthal angular correlations) for $Z=1, 2, 3,$ and 6 relative to the azimuthal direction of maximum collective momentum transfer in the flow plane ($\phi=0$) determined by the $Z=1,2$ particles (with autocorrelations removed). The left-hand column corresponds to peripheral collisions (MUL2) and the right-hand column to relatively central ones. The data are plotted for 200-MeV/nucleon Au+Au for two rapidity intervals (circles) $0.32 < y \leq 0.42$ and (crosses) $0.52 < y \leq 0.62$.

to rapidities of the emitted particles and fragments: near midrapidity $0.32 < y < 0.42$ (circles) and near-projectile rapidity $0.52 < y < 0.62$ (crosses), where the projectile rapidity is 0.64 . A strong azimuthal correlation is observed between all $Z \geq 2$ nuclei and the azimuthal direction of maximum collective momentum transfer in the flow plane, $\phi=0$. The correlation is rather flat for $Z=1$ and becomes increasingly stronger for heavier fragments. Projectile rapidity fragments are more correlated than midrapidity ones. The effect on projectile rapidity fragments is larger in central collisions than peripheral ones, whereas the midrapidity fragment correlations have very little dependence upon the centrality of the collision. In the limit of complete thermalization, azimuthally symmetric emission of midrapidity particles is expected. However, the presence of a correlation between fragments and the reaction plane suggests this picture is too simple; dynamic compression-decompression effects are present for the midrapidity fragments and high-multi-

plicity (central) events.

The observed correlations are predicted to arise from collective flow of matter in the collision. This should be more important for central collisions than peripheral ones, and a stronger correlation is indeed seen on the right-hand side of Fig. 3. The mass dependence of the correlation is also consistent with predictions of flow.¹¹⁻¹³ Fragment formation could result from the development of dynamic instabilities during expansion,²² or from a system in thermal and/or chemical equilibrium^{7,23,24} with additional dynamic effects, or from partial- or nonequilibrium processes. Studies of fragment flow may distinguish between these mechanisms. One might expect that the correlations from collective motion will be somewhat reduced by the random thermal motion generated in such energetic collisions. However, this is not always the case. For a system of nucleons and fragments in thermal equilibrium at a fixed freezeout temperature, the thermal energy is equally partitioned. Thus, the thermal energy per nucleon in a fragment of mass A has a $1/A$ dependence. The flow energy, which is originally compressional energy built up in the early stages of the collision, should have a linear A dependence, i.e., the compressional energy per nucleon is independent of A . The final fragment energy will be the sum of the thermal and flow energies. Thus, the flow energy is an increasingly larger fraction of the fragment energy and the thermal energy less important as the fragment mass A increases. The observations in Figs. 2 and 3 unambiguously demonstrate that the fragments exhibit stronger flow effects, both in momentum and position space, than do the lighter particles. Note, however, that it may not be possible to distinguish production of fragments in equilibrium models from coalescence of nucleons with use of the flow data alone, since the A dependence in both approaches is the same.²⁵

Results from the first large-solid-angle measurement of fragment formation in peripheral and central heavy-ion collisions have been presented. The events are characterized through the 4π measurement of the light charged particles, allowing the identification of multifragmentation events and analysis of the flow of the emitted nucleons and nuclear fragments. On the mean, eight to nine intermediate-mass fragments ($Z \geq 3$) are produced in central Au+Au collisions at 200 MeV/nucleon, with up to twenty possible. The transverse momentum per nucleon characterizing the flow and the alignment of the fragments both in position and momentum space relative to the reaction plane is observed to increase with the mass of the fragment. The observation of a stronger flow of fragments than that previously observed for light particles supports theoretical predictions of the existence of an enhanced collective flow of heavier nuclear fragments. This enhanced flow of fragments is particularly exciting as it may provide a more sensitive probe for future studies of the nuclear-matter equation of state.

The authors wish to thank G. Claesson, R. Ferguson, A. I. Gavron, and J. Wilhelmy for assistance during the experiment, H. Crawford for assistance in the in-beam fragment calibration tests, F. Lefebvres for his contributions to data analysis, and S. Chase for helpful comments in the preparation of this manuscript. The continuous support of R. Bock is gratefully acknowledged. Two of us (J.W.H. and A.M.P.) acknowledge support from the Alexander von Humboldt Foundation of West Germany during part of this work. This work was supported by the Director, Office of Energy Research, Division of Nuclear Physics of the Office of High Energy and Nuclear Physics of the U. S. Department of Energy under Contract No. DE-AC03-76SF00098.

^(a)Present address: Linear Accelerator Laboratory, University of Saskatchewan, Saskatoon, Saskatchewan, Canada S7N0W0.

^(b)Present address: University of Lund, Solvegation 14, S-22362 Lund, Sweden.

^(c)Permanent address: University of Münster, D-4400 Münster, West Germany.

¹H.-A. Gustafsson, H. H. Gutbrod, B. Kolb, H. Löhner, B. Ludewigt, A. M. Poskanzer, T. Renner, H. Riedesel, H.-G. Ritter, A. Warwick, F. Weik, and H. Wieman, *Phys. Rev. Lett.* **52**, 1590 (1984).

²R. E. Renfordt, D. Schall, R. Bock, R. Brockmann, J. W. Harris, A. Sandoval, R. Stock, H. Ströbele, D. Bangert, W. Rauch, G. Odyneic, H. G. Pugh, and L. S. Schroeder, *Phys. Rev. Lett.* **53**, 763 (1984).

³W. Scheid, H. Müller, and W. Greiner, *Phys. Rev. Lett.* **32**, 741 (1974).

⁴A. A. Amsden, G. F. Bertsch, F. H. Harlow, and J. R. Nix, *Phys. Rev. Lett.* **35**, 905 (1975).

⁵H. Stöcker, J. Maruhn, and W. Greiner, *Phys. Rev. Lett.* **44**, 725 (1980).

⁶H. Kruse, B. V. Jacak, and H. Stöcker, *Phys. Rev. Lett.* **54**, 289 (1985).

⁷J. Aichelin and H. Stöcker, *Phys. Lett.* **176**, 14 (1986).

⁸R. Y. Cusson, P. G. Reinhardt, J. J. Molitoris, H. Stöcker, M. Strayer, and W. Greiner, *Phys. Rev. Lett.* **55**, 2786 (1985).

⁹C. Gale, G. Bertsch, and S. DasGupta, *Phys. Rev. C* **35**, 1666 (1987).

¹⁰G. F. Bertsch, W. G. Lynch, and M. B. Tsang, *Phys. Lett. B* **189**, 384 (1987).

¹¹H. Stöcker, A. A. Ogloblin, and W. Greiner, *Z. Phys. A* **303**, 259 (1981).

¹²L. P. Csernai, H. Stöcker, P. R. Subramanian, G. Graebner, A. Rosenhauer, G. Buchwald, J. A. Maruhn, and W. Greiner, *Phys. Rev. C* **28**, 2001 (1983).

¹³L. P. Csernai, G. Fai, and J. Randrup, *Phys. Lett.* **140B**, 149 (1984).

¹⁴A. I. Warwick, H. H. Wieman, H. H. Gutbrod, M. R. Maier, J. Péter, H. G. Ritter, H. Stelzer, F. Weik, M. Freedman, D. J. Henderson, S. B. Kaufman, E. P. Steinberg, and B. D. Wilkins, *Phys. Rev. C* **27**, 1083 (1983).

¹⁵See also R. Bock, G. Claesson, R. L. Ferguson, H. A. Gustafsson, H. H. Gutbrod, A. I. Gavron, J. W. Harris, B. V. Jacak, K. H. Kampert, B. Kolb, A. M. Poskanzer, H. G. Ritter, H. R. Schmidt, T. Siemiarczuk, L. Teitelbaum, M. Tinncknell, S. Weiss, H. Wieman, and J. B. Wilhelmy, Gesellschaft für Schwerionenforschung Darmstadt mbH Report No. GSI-87-25, 1987 (to be published).

¹⁶A. Baden, H. H. Gutbrod, H. Löhner, M. R. Maier, A. M. Poskanzer, T. Renner, H. Riedesel, H. G. Ritter, H. Spieler, A. Warwick, F. Weik, and H. Wieman, *Nucl. Instrum. Methods* **203**, 189 (1982).

¹⁷R. Albrecht, H. W. Daus, H. A. Gustafsson, H. H. Gutbrod, K. H. Kampert, B. W. Kolb, H. Löhner, B. Ludewigt, A. M. Poskanzer, H. G. Ritter, R. Schulze, H. Stelzer, and H. Wieman, *Nucl. Instrum. Methods* **A245**, 82 (1986).

¹⁸K. G. R. Doss, H. A. Gustafsson, H. H. Gutbrod, B. Kolb, H. Löhner, B. Ludewigt, A. M. Poskanzer, T. Renner, H. Riedesel, H. G. Ritter, A. Warwick, and H. Wieman, *Phys. Rev. C* **32**, 116 (1985).

¹⁹P. Danielewicz and G. Odyneic, *Phys. Lett.* **157B**, 146 (1985).

²⁰K. G. R. Doss, H.-A. Gustafsson, H. H. Gutbrod, K.-H. Kampert, B. Kolb, H. Löhner, B. Ludewigt, A. M. Poskanzer, H. G. Ritter, H. R. Schmidt, and H. Wieman, *Phys. Rev. Lett.* **57**, 302 (1986).

²¹See K.-H. Kampert, thesis, University of Muenster, 1986 (unpublished).

²²B. Strack and J. Knoll, *Z. Phys. A* **315**, 249 (1984).

²³A. Z. Mekjian, *Phys. Rev. Lett.* **38**, 640 (1977), and *Phys. Rev. C* **17**, 1051 (1978).

²⁴G. Fai and J. Randrup, *Nucl. Phys.* **A404**, 551 (1983).

²⁵J. Gosset, H. H. Gutbrod, W. G. Meyer, A. M. Poskanzer, A. Sandoval, R. Stock, and G. D. Westfall, *Phys. Rev. C* **16**, 629 (1977).